Time-delayed feedback control of chaos in a GaAs/AlGaAs heterostructure

Yang Gui(杨癸)[1,†] and Zhao Xueting(赵雪婷)[2]

(1 College of Physics & Electrical Engineering, Anyang Normal University, Anyang 455000, China)
(2 College of Science, Hebei University of Engineering, Handan 056038, China)

Abstract: A theoretical model has been developed to study nonlinear behaviors in a GaAs/AlGaAs heterostructure. We show that the system can exhibit chaotic oscillations under transverse magnetic fields and an electric field. The time-delayed feedback method was applied to stabilize the unstable periodic orbits (UPOs) embedded in the chaotic attractor. A bifurcation specified by a successive decrease in the number of UPOs with delayed time and feedback strength was revealed, indicating the stabilization of UPOs under feedback control. Noticeably, the introduction of a feedback perturbation will sometimes induce chaotic states that do not exist in the unperturbed system.

Key words: chaos; feedback strength; delayed time
DOI: 10.1088/1674-4926/31/5/052003 **EEACC:** 2520

1. Introduction

Controlling chaos as a very active topic in nonlinear science has received extensive attention since the pioneering work of Ott, Grebogi, and Yorke (OGY)[1]. A variety of methods[1−6] have been suggested and applied to physical, chemical and biological systems for chaos control and synchronization[7−10]. The key of the OGY method[1] is to drive a UPO embedded in the chaotic attractors onto a stable target orbit by imposing an external force that is switched on only when the trajectory of the UPO moves to a sufficiently small vicinity of the target orbit. Thus, prior knowledge concerning the location and stability of the target orbit is required. Another famous approach was developed by Pyragas[6]. A brief introduction to it is given below. Consider a dynamical system that possesses chaotic states when the external controlling signal $f(t, y_i)$ is switched off. One can simulate the system by a set of ordinary equations,

$$\frac{\mathrm{d}y}{\mathrm{d}t} = P(y,t) + f(t), \tag{1}$$

$$f(t) = k[y_i(t-\tau) - y_i(t)] = kD(t). \tag{2}$$

Here y is the state vector, and y_i is a component of the state vector. Thus, the control signal (or the feedback perturbation) $f(t)$ imposed on the system is proportional to the amplitude of the selected component y_i subtracted from its preceding value $y(t-\tau)$ with a delayed time of τ seconds. k is known as perturbation strength. Clearly, the feedback perturbation vanishes when τ was adjusted to be precisely equal to the period T of a UPO embedded in the chaotic states, which implies that the system is likely to be stabilized onto the UPO of period T under the feedback control. That is, the stability of the preexisting unstable periodic orbits would vary while the orbit itself and its period remain unaltered with the perturbation parameters. This can be understood as follows: the introduction of the feedback perturbation in Eq. (1) expands the dimension of the unperturbed system to infinity. These extra degrees of freedom can be used to change the sign of the system Lyapunov exponents and to stabilize the UPOs. This approach is appealing for many workers since one does not need to know more information about the target orbit beyond its period T. In chaos theory, multiscroll chaotic systems[11−13] and the Lorenz system family[14] are important. This method has been extended to these systems[15,16] which show more interesting dynamical behaviors under feedback perturbation.

In this paper, the time-delayed feedback method is applied to a GaAs/AlGaAs heterostructure to stabilize the orbits embedded in the chaotic attractors. Two complementary cases are considered: (1) k is fixed while τ is changed; (2) τ is fixed and k is changed. Indeed, the system Lyapunov exponents change sign from positive to negative when the feedback strength k and delayed time τ vary in a certain range. The selected range allowed us to analyze the bifurcation of the system and to discover some regularity showed by the Poincaré map. It shows that "inverse-period-doubling" bifurcation firstly occurs in these two cases, implying that the system can be stabilized under feedback control. This was further demonstrated by investigating the response of the chaotic system to the delayed feedback perturbation with different parameters. We showed that the stabilized domain can be made reasonably large by carefully arranging the feedback controlling parameters k and τ. This would be potentially useful in engineering applications.

2. Model

The nonlinear transport of a modulation-doped GaAs/$Al_xGa_{1-x}As$ under a transverse magnetic field and an ac electric field is described by a set of differential equations that can be found in Ref. [17]. In this section, we give a brief introduction to the model. The sketch of the energy-band of the GaAs/$Al_xGa_{1-x}As$ heterostructure and the circuit diagram are shown in Figs. 1(a) and 1(b), respectively. The GaAs layer is undoped, while the AlGaAs layer is heavily n-doped with the donor density N_D. ΔE_c is the conduction band discontinuity. ϕ_b represents the interface potential barrier. μ_1 and μ_2 are the mobility of electrons at zero magnetic field in the GaAs and AlGaAs layers, respectively. The charge carrier density n, the interface potential barrier ϕ_b between the GaAs and AlGaAs lay-

† Corresponding author. Email: kuiziyang@126.com
Received 21 June 2009, revised manuscript received 12 December 2009

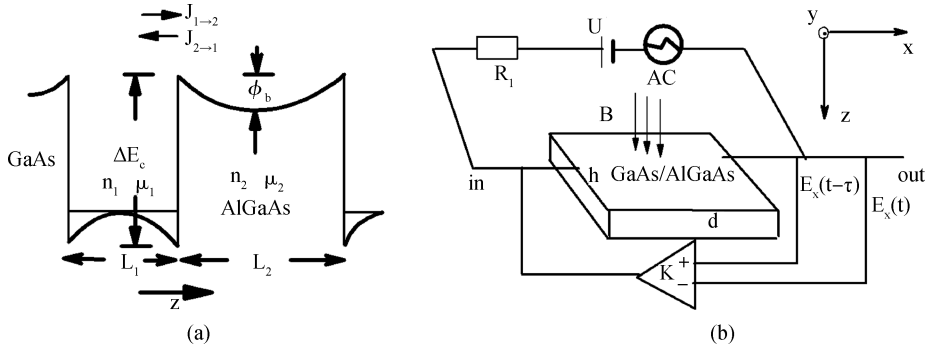

Fig. 1. (a) Energy-band diagram of GaAs/AlGaAs heterostructure with layer widths L_1 and L_2, and lateral dimensions h, and d. (b) Circuit diagram connected with the crossed magnetic field B and ac bias. The drift electric field E_x is used as the feedback component with the feedback strength k.

ers, and the electric field E are used as variables in the model.

Define the spatially averaged carrier densities in the GaAs and AlGaAs layers as $n_1 = \frac{1}{L_1}\int_{-L_1}^{0} n(z,t)\mathrm{d}z$ and $n_2 = \frac{1}{L_2}\int_{0}^{L_2} n(z,t)\mathrm{d}z$, respectively. Starting with the current continuity equation $\nabla \cdot J = -\partial\rho/\partial t$ and the conservation of the total number of carriers, we have,

$$\frac{\mathrm{d}n_1}{\mathrm{d}t} = \frac{J_{1\to2} - J_{2\to1}}{eL_1}, \tag{3}$$

$$n_1 L_1 + n_2 L_2 = N_{\mathrm{D}} L_2, \tag{4}$$

where

$$J_{1\to2} = -en_1\sqrt{\frac{E_1}{3\pi m_1^*}}\exp\frac{-3\Delta E_{\mathrm{c}}}{2E_1},$$

$$J_{2\to1} = -en_2\sqrt{\frac{E_2}{3\pi m_2^*}}\exp\frac{-3\phi_{\mathrm{b}}}{2E_2}.$$

$J_{1\to2}$ ($J_{2\to1}$) are the thermal emission current densities from the GaAs to AlGaAs (AlGaAs→GaAs) layers[18], respectively. The effective masses in the GaAs and AlGaAs layers are denoted as m_i^* ($i = 1, 2$). The mean energy as a function of the applied electric field E_x is approximately estimated by $E_i \approx E_{\mathrm{L}} + \tau_E e\mu_i E_x^2$, where τ_{E} is the energy relaxation time, $E_{\mathrm{L}} = (3/2)k_{\mathrm{B}}T_{\mathrm{L}}$ are the mean carrier energies, and T_{L} is the lattice temperature.

As for the formation of ϕ_{b}, an important feature is the ubiquitous presence of space charge[19]. This space charge induces a further feedback between the charge carrier distribution and the electric potential distribution via Poisson's equation. This mutual nonlinear interdependence is particularly pronounced in the case of low-dimensional structures, in which junctions between different layers on an atomic length scale cause conduction band discontinuities, resulting in interface potential barriers and wells.

Choose the drift electric field E_x as the feedback component. Dynamic equations of GaAs/ Al_x Ga_{1-x} As for the electric field read[20],

$$\dot{\phi_b} = \frac{e}{\varepsilon}\Big[-\mu_2 N_{\mathrm{D}}\phi_{\mathrm{b}} + \mu_2\frac{e^2}{2\varepsilon}L_1^2 n_1^2 - eL_1L_2\dot{n_1}\Big], \tag{5}$$

$$\varepsilon\dot{E_x} = \sigma_{\mathrm{l}}(E_x - E_u) + \sigma_{\mathrm{m}}E_x + \sigma_{\mathrm{n}}E_y + F(t), \tag{6}$$

Table 1. Model parameters used in this paper.

Parameter	Value
N_{D}	10^{17} cm^{-3}
μ_1	8000 cm^2/(V· s)
μ_2	50 cm^2/(V· s)
ΔE_{c}	250 meV
h	1 mm
τ_{E}	5.0×10^{-12} s
ε	$12\varepsilon_0$
ε_0	8.854×10^{-12} F/m
k_{B}	1.380×10^{-23} J·K
L_1	10 nm
L_2	20 nm
T_{l}	300 K
m_1^*	$0.067m_0$
m_2^*	$(0.067 + 0.083\times0.3)m_0$
d	50 μm
m_0	0.91×10^{-30} kg
R_{l}	1144 Ω
V_{ds}	5.0×10^7 m/s

$$\varepsilon\dot{E_y} = \sigma_{\mathrm{m}}E_y + \sigma_{\mathrm{n}}E_x, \tag{7}$$

where $\sigma_{\mathrm{l}} = -d/(h(L_1 + L_2)R_{\mathrm{l}})$, $\sigma_{\mathrm{m}} = -(en_1\mu_{1\mathrm{B}}L_1 + en_2\mu_{2\mathrm{B}}L_2)/(L_1 + L_2)$, and $\sigma_{\mathrm{n}} = -eB(n_1\mu_{1\mathrm{B}}\mu_1L_1 + n_2\mu_{2\mathrm{B}}\mu_2L_2)/(L_1 + L_2)$. ε is the permittivity. The field dependences of the mobility for the two layers are given by $\mu_{iB} = \mu_i/(1 + \mu_i^2B^2)$, $i = 1, 2$, respectively. The values of the model parameters used in this paper are listed in Table 1. A static magnetic field in the Z direction is expressed as $B = B\hat{Z}$, and the applied electric field is denoted as $E_{\mathrm{u}} = U_0(1 + A\sin(2\pi nf_0t))/d$. The dimensionless variables are defined as: $Y_1 = n_1/N_{\mathrm{D}}$, $Y_2 = \mu_1E_x/V_{\mathrm{ds}}$, $Y_3 = \mu_1E_y/V_{\mathrm{ds}}$, $Y_4 = \phi_{\mathrm{b}}/(k_{\mathrm{B}}T_{\mathrm{l}})$, and $T = t/\tau_{\mathrm{E}}$. The fourth order Runge–Kutta technique is used in our numerical simulations.

In this model, we have neglected the diffusive contributions that have to be included only when the GaAs/AlGaAs layer-thickness is much larger than the mean free path of the electrons. Quantum effects like the quantum-transmission coefficient or tunneling through the barrier are also ignored[21]. In addition, quantum size effects are neglected since the current–voltage characteristic is almost independent of the quasi-two-dimensional subbands below the barrier when the layer thickness is greater than 100 Å.

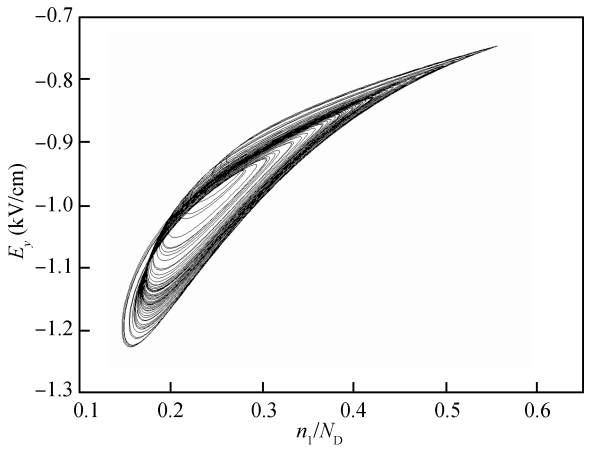

Fig. 2. Chaotic phase portrait of the unperturbed system onto the (n_1, E_y) plane.

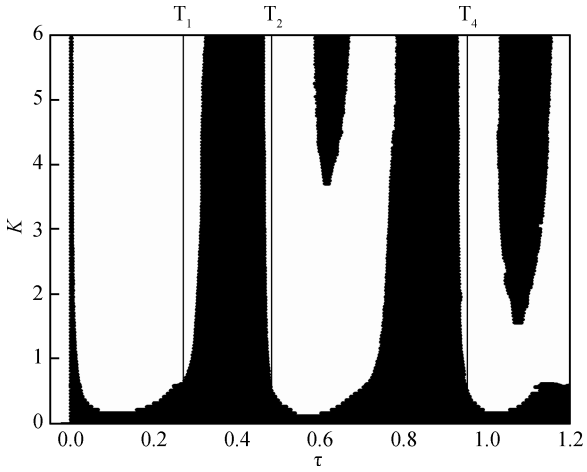

Fig. 3. Maximal Lyapunov exponent of the system varying with feedback parameters (τ, k).

3. Simulations and discussions

As we set the amplitude $A = 0$, the system shows self-sustained oscillations which can be understood as follows. As the electric field increases, the electrons in the GaAs layer will get enough kinetic energy which is higher than ΔE_c to tunnel across the barrier into the AlGaAs layer, which is similar to thermionic emission from the GaAs layer into the doped AlGaAs layer. This causes an increase of carrier density in the AlGaAs layer which has several consequences. First, since the carrier mobility μ_2 in the AlGaAs layer is much lower than μ_1 in the undoped GaAs layer, according to the current density $J_x = eE_x(n_1\mu_1 L_1 + n_2\mu_2 L_2)/(L_1 + L_2)$ and Eq. (4), an increase of the carrier density n_2 in the AlGaAs layer also implies some decrease of the longitudinal current density. Second, the potential barrier ϕ_b will decrease with some delay due to the finite dielectric relaxation time, which leads then to an increased backward current with some reduction of the carrier density in the AlGaAs, which, in turn, depresses the backward thermionic emission current, forming complete cycles of real-space charge transfer. Thus self-sustained oscillation occurs and the frequency $f_0 = 90.744$ GHz. As a result of the competition between the internal signal and the external signal, the system shows different oscillating modes like chaos frequency-locking and quasiperiodicity depending on the relative amplitude A and the driving frequency. A detailed description is given in Ref. [17].

In this section, we first set the feedback strength $k = 0$. We choose the magnetic field $B = 0.3$ T, and $U_0 = 39.25$ V, and the ac electric field with a relative amplitude $A = 0.08$ and the frequency of nf_0 with $n = 9.5$ so that the system is in the chaotic state. The corresponding chaotic phase portrait in the (n_1, E_y) plane is shown in Fig. 2. For this nonautonomous system, the periods of UPOs embedded into the chaotic attractor are then measured by $T_i = i/(9.5f_0), i = 1, 2, \ldots$.

We switch on the time-delayed feedback perturbation to control the chaotic system. We find that sign change in the system Lyapunov exponents occurs as the feedback strength k and the delayed time τ vary. The feedback parameter (τ, k) dependences of the maximal Lyapunov exponent of the perturbed system are shown in Fig. 3. In this figure, the shadows mark the regimes where the values of the Lyapunov exponent are positive, which then means the system is in the chaotic state. The vertical bold solid lines $\tau = T_i$ $(i = 1, 2, 4)$ correspond to the periods of unstable periodic states embedded into the chaotic attractors. Indeed, the UPOs with period T_i can be stabilized, except for a very weak feedback strength k, as expected.

The bifurcation of the system is further investigated by varying the feedback parameters. For better visualization, we use the Poincaré map technique and consider two complementary cases. The E_y projection of the Poincaré map orbit obtained by sampling the trajectory every $T = 1/(nf_0)$ seconds is plotted in Figs. 4(a)–4(d). Panels (a) and (b) denote the case of two fixed τ values and an "inverse-period-doubling" bifurcation come into being with the varied k. For $\tau = T_1$ (Fig. 4(a)), a period-4 orbit can be stabilized for the perturbation strength k in the range of $0.63 < k < 1.31$. For $1.31 \leqslant k \leqslant 4.28$, however, period-2 orbit is under control. Note that the system is stabilized while the feedback signal does not vanish until the feedback time τ is equal to the period of period-1. Further increasing k, period-1 orbit becomes stable and the feedback perturbation disappears. A similar process is shown in Fig. 4(b) for $\tau = T_2$. It follows from Figs. 4(a) and 4(b) that a large feedback strength would lead to greater freedom in selecting the delayed time; that is, a wider region of controlling parameters where UPOs can be stabilized.

We discuss the delay time τ-dependence of the bifurcation for fixed feedback strength. It can be seen from both panels (c) for $k = 0.6$ and (d) for $k = 3.0$ that the dynamic behaviors of the system become more complex. As shown in Fig. 4(c), the system is firstly driven onto a period state as τ increases from 0 to 0.132. Then, the system undergoes a period-doubling bifurcation from the periodic orbit to the chaotic state when the delay time τ falls in the range of $(0.132, 0.33)$. Similar bifurcation scenarios appear consecutively as the delayed time τ sweeping from small to large values. We plot the phase portrait of the induced chaotic states onto the (n_1, E_y) plane in Fig. 5(a) and the temporal evolution of the electric field E_y in Fig. 5(b), respectively. The inset in Fig. 5(a) displays the chaotic states without feedback control. Clearly, a delayed feedback with appropriate parameters k and τ is able to stabilize the UPOs em-

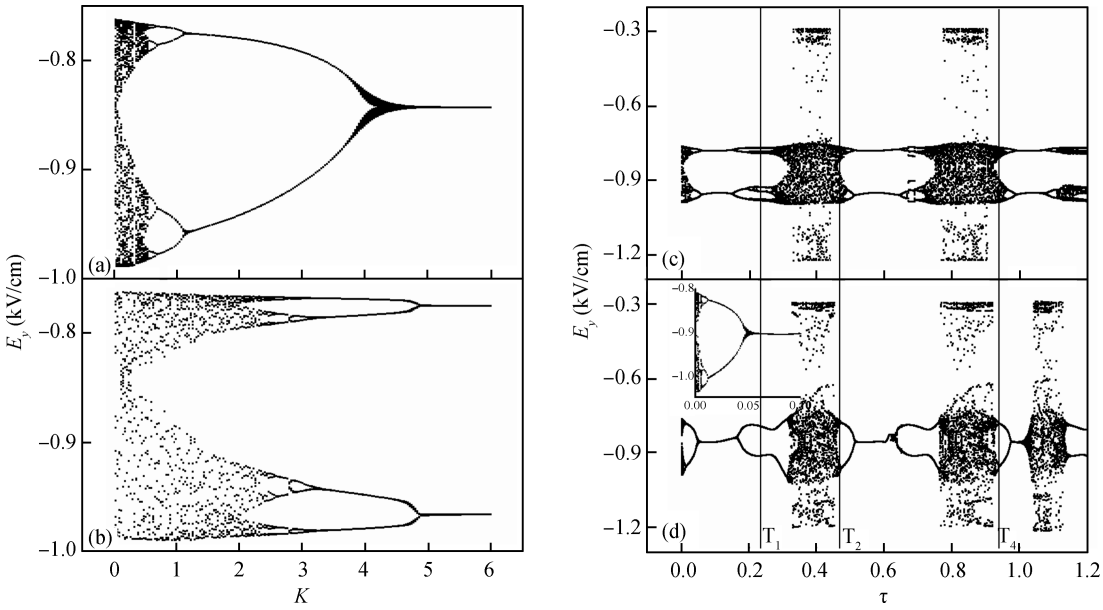

Fig. 4. Bifurcation diagram of the Poincaré map orbit versus perturbation parameters k and τ for fixed (a) $\tau = T_1$ and (b) $\tau = T_2$, and for (c) $k = 0.6$ and (d) $k = 3.0$, respectively. The vertical solid lines mark the periods of some unstable periodic states, such as T_1, T_2, and T_4.

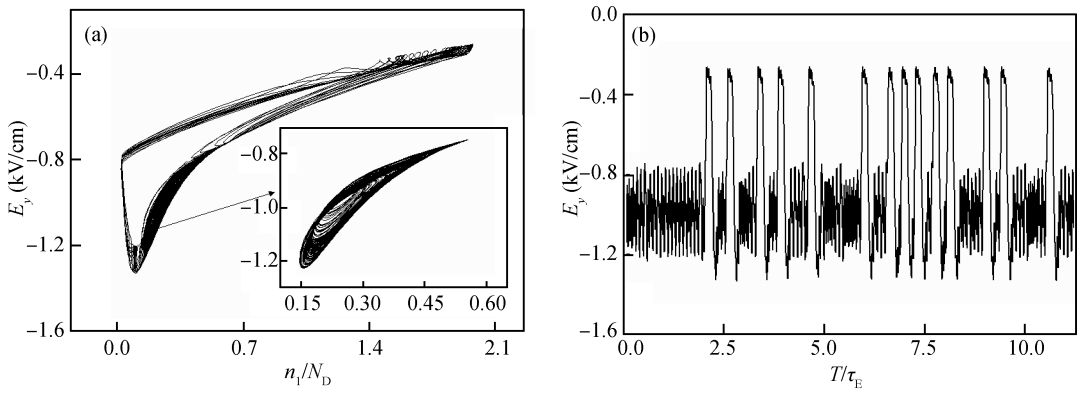

Fig. 5. Chaotic states induced by the feedback perturbation. (a) Phase portrait in the (n_1, E_y) plane. (b) Temporal evolution of the electric field E_y.

bedded into the chaotic attractors. Meanwhile, it would possibly lead to a cascade of period-doubling bifurcation of chaos. The same phenomenon has been reported in Refs. [22, 23]. One must be careful in selecting the perturbation parameters for chaos control.

We show the temporal evolution of the system output in Figs. 6(a)–6(d) for different values of the feedback strength k and delayed time τ. In each panel, the upper plot shows the perturbation signal $F(t)$ together with an inset that denotes the system phase portrait in the (n_1, E_y) plane, whereas the lower plots the electric field E_y versus time. It is illustrated that the feedback output became steadily weaker when the feedback control was switched on, and it finally faded out after a short period of transient time. Simultaneously, the system was stabilized onto some UPOs. Figure 6(a) demonstrates the case without the controlling term i.e. $k = 0$. The projection of the phase portrait in the (n_1, E_y) plane shows that the system exhibits chaotic oscillations. In Figs. 6(b), 6(c), and 6(d), we show the stable period-i ($i = 1, 2, 4$) orbit under different control parameters.

4. Conclusions

We have discussed the effects of time-delayed feedback control on the dynamic behaviors of a GaAs/AlGaAs heterostructure that can exhibit unstable orbits or chaotic states. The general structure of the bifurcation diagram of the system is discovered which is dependent upon two feedback parameters. To explore the system behaviors, Lyapunov exponents are considered as functions of feedback perturbation parameters. The delayed time τ is chosen from 0 up to 1.2 (longer than the period of period-4 UPO in the unperturbed system), and the feedback strength k is in the range of $1.31 \leqslant k \leqslant 4.28$, which is sufficiently wide for the present work. It shows that the system Lyapunov exponents can change sign from positive to negative when the feedback strength k and delayed time τ vary in a certain range, and the system is stabilized onto some unstable periodic orbits under the feedback control, accordingly. Several domains are found where stabilization of UPOs is possible, besides those in the neighborhood of $\tau = T_i s$. On the other hand, the chaotic states may occur when $\tau \neq T_i$, which

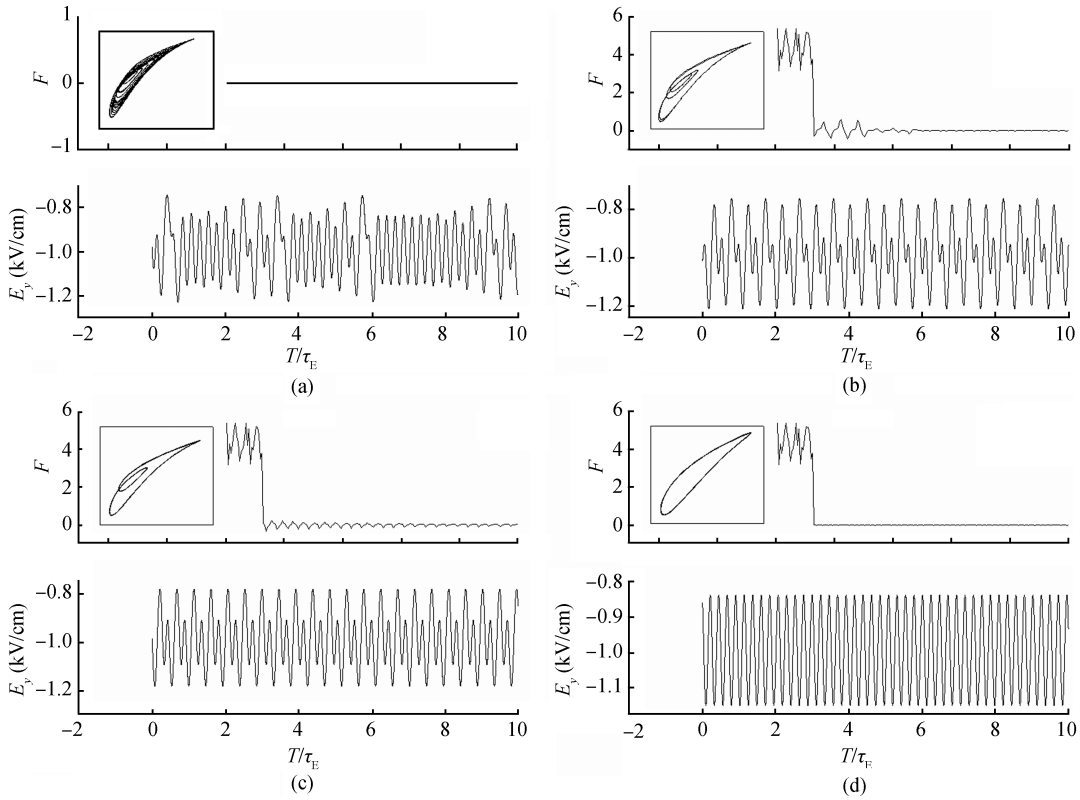

Fig. 6. Dynamical behaviors of the perturbed system at different control parameters. (a) $k = 0$. (b) $k = 4, \tau = T_4$. (c) $k = 5.2, \tau = T_2$. (d) $k = 4.3, \tau = T_1$.

is in good agreement with work by other groups[22−26].

References

[1] Ott E, Grebogi C, Yorke J A. Controlling chaos. Phys Rev Lett, 1990, 64: 1196

[2] Schuster H G. Handbook of chaos control. Weinheim: Wiley-VCH, 1999

[3] Boccaletti S, Grebogi C, Lai Y C, et al. The control of chaos: theory and applications. Phys Rep, 2000, 329: 103

[4] Gauthier D J. Resource letter: CC-1: controlling chaos. Am J Phys, 2003, 71: 750

[5] Hbinger B, Doerner R, Martienssen W. Local control of chaotic motion. Z Phys B, 1993, 90: 103

[6] Pyragas K. Continuous control of chaos by self-controlling feedback. Phys Lett A, 1992, 170: 421

[7] Hövel P, Schöll E. Control of unstable steady states by time-delayed feedback methods. Phys Rev E, 2005, 72: 046203

[8] Schlesner J, Amann A, Janson N B, et al. Self-stabilization of high-frequency oscillations in semiconductor superlattices by time-delay autosynchronization. Phys Rev E, 2003, 68: 066208

[9] Pyragas V, Pyragas K. Delayed feedback control of the Lorenz system: an analytical treatment at a subcritical Hopf bifurcation. Phys Rev E, 2006, 73: 036215

[10] Yamasue K, Hikihara T. Conservative chaotic map as a model of quantum many-body environment. Phys Rev E, 2006, 73: 036209

[11] Yu S M, Lü J H, Chen G R. Theoretical design and circuit implementation of multidirectional multi-torus chaotic attractors. IEEE Trans Circuits Syst I, 2007, 54(9): 2087

[12] Lü J H, Chen G R. Multi-scroll chaos generation: theories, methods and applications. Int J Bifurcation Chaos, 2006, 16(4): 775

[13] Lü J H, Yu S M, Leung H, et al. Experimental verification of multidirectional multiscroll chaotic attractors. IEEE Trans Circuits Syst I, 2006, 53(1): 149

[14] Lü J H, Chen G R. A new chaotic attractor coined. Int J Bifurcation Chaos, 2002, 12(3): 659

[15] Wang L, Ni Q, Huang Y Y. Dynamical behaviors of Liu system with time delayed feedback. Journal of Dynamics and Control, 2007, 5(3): 224 (in Chinese)

[16] Li J, Zhou J L, Wang Y, et al. Synchronization of N-scroll hyperchaotic attractors. Signal Processing, 2007, 23(3): 408 (in Chinese)

[17] Yang G, Zhao H, Zhou S. The dynamics and hysteresis in GaAs/AlGaAs heterostructure under the action of electric and magnetic fields. Mod Phys Lett B, 2008, 22: 425

[18] Hess K. Advanced theory of semiconductor devices. New Jersey: Prentice Hall, 1988

[19] Schöll E. Nonlinear spatio-temporal dynamics and chaos in semiconductors. Cambridge: Cambridge University Press, 2001

[20] Hüpper G, Schöll E. Dynamic Hall effect as a mechanism for self-sustained oscillations and chaos in semiconductors. Phys Rev Lett, 1991, 66: 2372

[21] Glisson T H, Hauser J R, Littlejohn M A, et al. Monte Carlo simulation of real-space electron transfer in GaAs-AlGaAs heterostructures. J Appl Phys, 1980, 51: 5445

[22] Xu J, Chung K W. Effects of time delayed position feedback on a van der Pol–Duffing oscillator. Physica D, 2003, 180: 17

[23] Kociuba G, Heckenberg N R. Controlling chaos in a Lorenz-like system using feedback. Phys Rev E, 2003, 68: 066212

[24] Balanov A G, Janson N B, Schöll E. Delayed feedback control of chaos: Bifurcation analysis. Phys Rev E, 2005, 71: 016222

[25] Nakajima H. On analytical properties of delayed feedback control of chaos. Phys Lett A, 1997, 232: 207

[26] Just W, Bernard T, Ostheimer M, et al. Mechanism of time-delayed feedback control. Phys Rev Lett, 1997, 78: 203